



<b>Publication Year</b>	2020
<b>Acceptance in OA</b>	2022-06-20T09:21:34Z
<b>Title</b>	Search for ${}^7\text{Be}$ in the outbursts of four recent novae
<b>Authors</b>	MOLARO, Paolo, Izzo, L., Bonifacio, P., Hernanz, M., Selvelli, P., DELLA VALLE, Massimo
<b>Publisher's version (DOI)</b>	10.1093/mnras/stz3587
<b>Handle</b>	<a href="http://hdl.handle.net/20.500.12386/32405">http://hdl.handle.net/20.500.12386/32405</a>
<b>Journal</b>	MONTHLY NOTICES OF THE ROYAL ASTRONOMICAL SOCIETY
<b>Volume</b>	492



# Search for $^7\text{Be}$ in the outbursts of four recent novae

P. Molaro <sup>1,2</sup>★, L. Izzo <sup>3,4</sup>, P. Bonifacio <sup>5</sup>, M. Hernanz <sup>6</sup>, P. Selvelli<sup>1</sup>  
and M. della Valle<sup>7</sup>

<sup>1</sup>INAF-Osservatorio Astronomico di Trieste, Via G.B. Tiepolo 11, I-34143 Trieste, Italy

<sup>2</sup>Institute of Fundamental Physics of the Universe, Via Beirut 2, 34151, Grignano, Trieste, Italy

<sup>3</sup>Instituto de Astrofísica de Andalucía, Glorieta de la Astronomía s/n, 18008, Granada, Spain

<sup>4</sup>DARK Cosmology Centre, Niels Bohr Institutet, Københavns Universitet, Lyngbyvej 2, 2100 København, Denmark

<sup>5</sup>GEPI, Observatoire de Paris, Université PSL, CNRS, Place Jules Janssen, 92195 Meudon, France

<sup>6</sup>Institute of Space Sciences (ICE, CSIC) and IEEC, Campus UAB, Camí de Can Magrans s/n, 08193 Cerdanyola del Valles (Barcelona), Spain

<sup>7</sup>Capodimonte Astronomical Observatory, INAF-Napoli, Salita Motariello 16, 80131-Napoli, Italy

Accepted 2019 December 18. Received 2019 December 18; in original form 2019 August 14

## ABSTRACT

Following the recent detection of  $^7\text{Be II}$  in the outburst spectra of classical novae, we report the search for this isotope in the outbursts of four recent bright novae by means of high-resolution Ultraviolet and Visual Echelle Spectrograph (UVES) observations. The  $^7\text{Be II } \lambda\lambda 313.0583, 313.1228$  nm doublet resonance lines are detected in the high-velocity components of Nova Mus 2018 and ASASSN-18fv during outbursts. However,  $^7\text{Be II}$  is not detected in ASASSN-17hx and possibly not in Nova Cir 2018, which shows that  $^7\text{Be}$  is not always ejected in the thermonuclear runaway. Taking into account the  $^7\text{Be}$  decay, we find  $X(^7\text{Be})/X(\text{H}) \approx 1.5 \times 10^{-5}$  and  $2.2 \times 10^{-5}$  in Nova Mus 2018 and ASASSN-18fv, respectively. A value of  $^7\text{Be}/\text{H} \approx 2 \times 10^{-5}$  is found in five out of the seven extant measurements, and it can be considered as a typical  $^7\text{Be}$  yield for novae. However, this value is almost one order of magnitude larger than predicted by current theoretical models. We argue that the variety of high  $^7\text{Be}/\text{H}$  abundances could be the result of a higher than solar content of  $^3\text{He}$  in the donor star. The cases with  $^7\text{Be}$  not detected might be related to the small mass of the white dwarf (WD) or to relatively little mixing with the core material of the WD. The  $^7\text{Be}/\text{H}$ , or  $^7\text{Li}/\text{H}$ , abundance is  $\approx 4$  dex above meteoritic abundance, thus confirming the novae as the main sources of  $^7\text{Li}$  in the Milky Way.

**Key words:** nuclear reactions, nucleosynthesis, abundances – stars: individual: ASASSN-17hx – stars: individual: Nova Mus 2018 – stars: individual: Nova Cir 2018 – stars: individual: ASASSN-18fv – novae – Galaxy: evolution.

## 1 INTRODUCTION

In models of classical novae, hydrogen-rich material is transferred from a main-sequence star or evolved giant through an accretion disc on to a white dwarf (WD). The temperature on the WD surface rises until CNO cycle fusion starts (Starrfield, Iliadis & Hix 2016). It has been suggested that in the thermonuclear runaway  $^7\text{Be}$  could also be made via the reaction  $^3\text{He}(\alpha, \gamma)^7\text{Be}$  and then ejected (Arnould & Norgaard 1975; Starrfield et al. 1978).  $^7\text{Be}$  is a radioactive nucleus and decays into  $^7\text{Li}$  with a half-life of 53.22 d, so that all  $^7\text{Be}$  is expected to decay into  $^7\text{Li}$ . This suggestion dates back to the 1970s but it has been thwarted by the non-detection of  $^7\text{Li}$  (Friedjung 1979). The long-sought  $^7\text{Li I } \lambda\lambda 670.8$  nm resonance line was

recently identified in the slow nova V1369 Cen (Izzo et al. 2015). However, the resonance doublet of the parent nucleus  $^7\text{Be II}$  was detected in few novae (Tajitsu et al. 2015, 2016; Molaro et al. 2016; Izzo et al. 2018a). By re-analysis of historical novae using archival *International Ultraviolet Explorer (IUE)* observations,  $^7\text{Be II}$  has also been detected in emission in the very fast nova V838 Her (Selvelli, Molaro & Izzo 2018). This detection shows that  $^7\text{Be}$  is freshly created in the nova thermonuclear runaway and ejected in the outburst. It must be noted that in all these cases  $^7\text{Li I}$  at  $\lambda\lambda 670.8$  nm went undetected. So far,  $^7\text{Li I}$  has been detected only in V1369 Cen while the parent nuclei  $^7\text{Be}$  has been detected in all the novae where it has been searched for. The persistent non-detection of neutral  $^7\text{Li}$  after more than a decaying time has been explained by the capture of a K-shell electron by  $^7\text{Be}$ , thus transforming into  $^7\text{Li II}$ , which does not neutralize throughout the time of the outburst (Molaro et al. 2016).

\* E-mail: [paolo.molaro@inaf.it](mailto:paolo.molaro@inaf.it)

The  ${}^7\text{Be II } \lambda\lambda 313.1$  nm doublet shows a huge equivalent width (EW), comparable only to hydrogen and much greater than all other elements. The measured atomic fraction implies massive  ${}^7\text{Be}$  ejecta with the final  ${}^7\text{Li}$  product up to four and even five orders of magnitude above meteoritic abundance. With such an overproduction, novae could be an important  ${}^7\text{Li}$  factory exceeding by far what was synthesized in the big bang, or by other sources such as spallation by cosmic rays and asymptotic giant branch (AGB) stars. The role of novae as  ${}^7\text{Li}$  producers has been considered by Cescutti & Molaro (2019), who used a detailed model of the chemical evolution of the Milky Way. They have shown that novae account well for the observed increase of Li abundance with metallicity in the Galactic thin disc and also for the relative flatness observed in the thick disc. The latter evolves on a time-scale that is shorter than the typical time-scale in which novae produce substantial  ${}^7\text{Li}$ , and therefore does not show any enhancement.

A major problem is that the abundances measured exceed what is foreseen by current models (Hernanz et al. 1996; José & Hernanz 1998). Initially,  ${}^7\text{Be}$  detection occurred in slow novae, but it has also been found in fast novae such as V407 Lup, whose progenitor is likely an ONe WD (Izzo et al. 2018a), and V838 Her, which is one of the fastest ever observed (Selvelli et al. 2018). Thus, it seems that  ${}^7\text{Be}$  is present in both fast and slow novae and with comparable abundances.

The decay of  ${}^7\text{Be}$  produces a high-energy line at 478 keV emitted during the de-excitation to the ground state of the fresh  ${}^7\text{Li}$  produced in the  ${}^7\text{Be}$  electron capture (Gomez-Gomar et al. 1998). Several unsuccessful attempts to detect the line with gamma ray satellites have been performed (Harris et al. 2001). The detection of the radioactive  ${}^7\text{Be}$  nuclei in the nova outburst reopened the possibility of detectability of the 478-keV line with *INTEGRAL* for nearby novae. The distance should be less than  $\approx 0.5$  kpc, although the horizon will depend on the amount of  ${}^7\text{Be}$  produced in the nova event (Siegert et al. 2018). The nova ASASSN-18fv was observed with *INTEGRAL*-Director Discretionary Time, during 2.8 ms. Although the complete data analysis is still ongoing, it is already clear that only upper limits to the 478-keV emission line have been obtained, which are not constraining for the models (Siegert et al., in preparation).

Following the recent detection of  ${}^7\text{Be II}$  in the outburst spectra of classical novae, we activated a Target of Opportunity (ToO) programme at the European Southern Observatory (ESO) to target  ${}^7\text{Be}$  in novae that, at maximum, reach magnitude  $V \leq 9$ . We report here on the search for the  ${}^7\text{Be}$  isotope in high-resolution Ultraviolet and Visual Echelle Spectrograph (UVES) spectra of four recent novae discovered in the years 2017 and 2018.

## 2 THE PROGRAM NOVAE

The four novae of this programme have been the brightest novae since 2017. Source brightness is required in order to study the resonance doublet lines  ${}^7\text{Be II}$  that lie at  $\lambda\lambda 313.1$  nm, very close to the atmospheric cut-off where a significant atmospheric absorption is present.

Several UVES spectra for each nova were obtained following the maximum. The UVES settings were DIC1 346–564, with a central wavelength of 346 nm (range 305–388 nm) in the blue arm, to cover the  ${}^7\text{Be II } \lambda\lambda 313.1$  nm lines, and 564 nm (460–665 nm) in the red arm. Every observation was followed by another with the setting DIC2 437–760, to cover in the blue arm the H&K Ca II lines and in the red arm to cover several metallic lines and the  ${}^7\text{Li I}$  at  $\lambda\lambda 670.8$  nm. The journal of observations for each nova is provided

**Table 1.** Journal of observations. Only DIC1 settings are reported. Corresponding to each DIC1 setting, several DIC2 setting observations were taken with high resolution.

MJD	Day (a.m.)	exp (s) 346 nm	$R/1000$	exp (s) 564 nm	$R/1000$
ASASSN-17hx					
57980.0830	15	1100	71	1100	107
57988.0978	23	1100	50	1100	52
58013.0586	48	1100	50	1100	52
58056.0242	91	1100	71	1100	107
NOVA MUS 2018					
58134.3246	0	1200	50		
58134.3246		300	50		
58169.0644	35	800	52	800	52
58169.0877		600	50	600	52
58169.0952		600	50	600	52
58174.1406	40	1200	50	1200	52
58178.1866	44	1200	50	1200	52
NOVA CIR 2018					
58142.3528	−15	60	71	60	107
58142.3542		300	71	300	107
58150.2844	−7	600	59	600	66
58169.2516	12	600	50	600	52
58169.2598		200	50	200	52
58169.2627		200	50	200	52
58169.2656		200	50	200	52
58177.1187	20	600	50	2x250	52
58181.3439	24	600	50	2x250	52
58187.1453	30	600	50	2x250	52
58191.3409	34	600	50	250	52
58215.1463	58	600	59	120	66
58220.1456	63	600	59	120	66
58223.1423	66	600	59	60	66
58227.9869	71	300	59	60	66
58232.2215	75	300	59	120	66
58232.2136		600	59	120	66
58232.2054		600	59	120	66
58243.0936	86	600	59	60	66
ASASSN-18fv					
58199.1438	−7	60	59	60	66
58199.1452		300	59	300	66
58201.1412	−5	300	59	60	66
58203.0924	−3	300	59	60	66
58205.0687	−1	300	59	60	66
58207.0599	1	600	59	120	66
58209.0218	3	600	59	120	66
58213.0665	7	600	59	120	66
58215.1292	9	600	59	120	66
58217.0686	11	600	59	120	66
58220.1292	14	600	59	120	66
58223.1262	17	600	59	60	66
58227.9869	21	300	59	15	66
58228.0002	22	150	59	30	66
58228.0043		50	59	6	66
58235.9959	29	300	59	60	66
58249.0205	43	600	59	120	66
58262.1078	56	600	59	120	66
58280.0381	74	1200	59	3x224	66
58285.9707	80	1200	59	120	66
58303.9851	98	1400	59	13x60	66

in Table 1. The resolving power was typically  $R = \lambda/\delta\lambda \approx 80\,000$  for the blue arm and  $\approx 120\,000$  for the red arm. Overlapping spectra have been combined for each epoch to maximize the signal-to-noise ratio.

**Table 2.** A list of single-ionized ions that are the main contributors to the absorption in the region around  $\lambda 313.0$  nm. Atomic data are taken from the NIST Lines data base. Those for Cr II are from Lawler et al. (2017).

Wavelength (Air) (nm)	Ion	Log(gf)	Low en. (eV)	Upper en. (eV)
311.0672	Ti II	-0.953	1.23	5.21
311.2049	Ti II	-1.157	1.22	5.21
311.4295	Fe II	-1.43	3.89	7.87
311.658	Fe II	-1.50	3.89	7.87
311.7666	Ti II	-0.494	1.23	5.21
311.8649	Cr II	-0.08	2.42	6.40
311.9799	Ti II	-0.485	1.24	5.22
312.0369	Cr II	0.10	2.43	6.41
312.4978	Cr II	0.26	2.45	6.42
312.8700	Cr II	-0.53	2.43	6.40
313.0583	Be II	-0.178	0.00	3.96
313.1228	Be II	-0.479	0.00	3.96
313.2056	Cr II	0.43	2.48	6.44
313.3048	Fe II	-1.9	3.89	7.84
313.6681	Cr II	-0.44	2.45	6.41

The  $^7\text{Be}$  II resonance lines are at 313.1 nm in a particularly challenging region, because of both the Earth’s atmosphere absorption and the transmission optical components of the spectrographs. The identification was made using the close correspondence in the position of the  $^7\text{Be}$  II lines with that of other ions that are known to be present in the outburst spectra. Coincidences are always possible and the most strong lines in the  $^7\text{Be}$  region are listed in Table 2. The detection becomes robust only when the other line of the  $^7\text{Be}$  resonance doublet at 313.1228 nm is also visible. Unfortunately, narrow components are not always present in the outburst spectra. When seen, the UVES resolution of  $\approx 4 \text{ km s}^{-1}$  allows us to distinguish even between  $^7\text{Be}$  and  $^9\text{Be}$  isotopes.  $^9\text{Be}$  transitions fall at  $\lambda\lambda 313.04219$  and  $313.10667$  nm at  $15.6 \text{ km s}^{-1}$  from the lighter isotope. However,  $^9\text{Be}$  is not synthesized in the nova thermonuclear runaway and, if present, it would be the one from the companion at a level of  $^9\text{Be}/\text{H} = 2.4 \times 10^{-11}$  (Lodders, Palme & Gail 2009). Such a small abundance would be undetectable in the outburst spectra and  $^7\text{Be}$  is found at an abundance of six orders of magnitude higher.

## 2.1 Nova ASASSN-17hx

ASASSN-17hx was discovered on 2017 June 19 (Stanek et al. 2017a,b,c) in the Scutum constellation by the All-Sky Automated Survey for SuperNovae (ASASSN; Shappee et al. 2014). Initially of  $V = 12$  mag, ASASSN-17hx brightened continuously to reach  $V \approx 8$  mag on 2017 July 31. The nova showed a long pre-maximum plateau. This is characteristic of slow novae and produced by an optically thick expanding envelope that undergoes cooling during the expansion. After peak, the nova declined and re-brightened several times up to 100 d after maximum. The detailed light curve of ASASSN-17hx is shown in Fig. 1. The nova was initially classified as a He/N nova, but later developed strong Fe II features, thus showing features of both He/N and Fe II novae at different epochs (Guarro et al. 2017; Munari et al. 2017; Pavana et al. 2017; Williams & Darnley 2017; Poggiani 2018). ASASSN-17hx is at low Galactic latitude ( $b = -2^\circ.22442$ ) and it is highly reddened. The reddening maps of Schlafly & Finkbeiner (2011) provide  $E(B - V) = 1.565$  mag while those of Schlafly, Finkbeiner & Davis (1998) provide  $E(B - V) = 1.820$  mag; the latter value becomes  $E(B - V) = 1.218$  mag when corrected according to the prescription of Bonifacio,

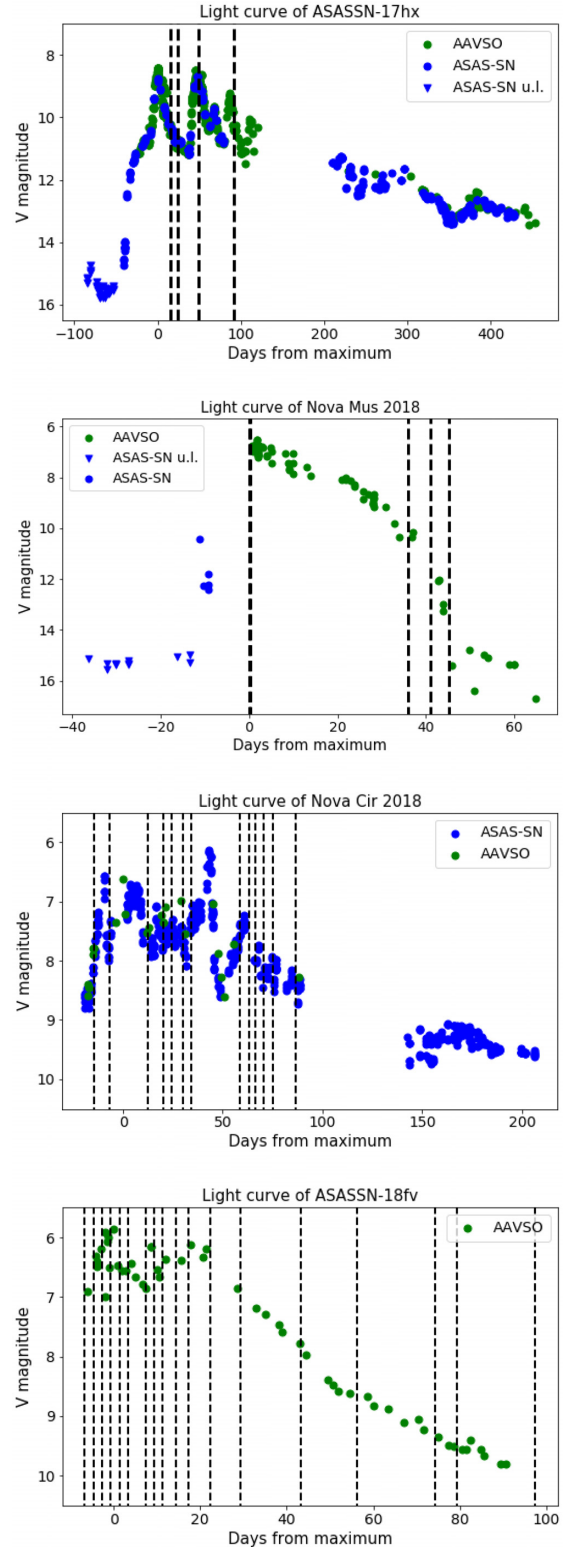


**Figure 1.** V-band light curves of the four novae described in this paper, obtained using data from ASASSN and the American Association of Variable Star Observers (AAVSO) data base. From the top, we show ASASSN-17hx, Nova Mus 2018, Nova Cir 2018 and ASASSN-18fv. Vertical lines mark our spectroscopic observations. The maximum epoch for each nova has been computed from AAVSO data. These are JD 245 7964.4886 for ASASSN-17hx, JD 245 8134.8891 for Nova Mus 2018, JD 245 8157.0024 for Nova Cir 2018 and JD 245 8205.9593 for ASASSN-18fv.

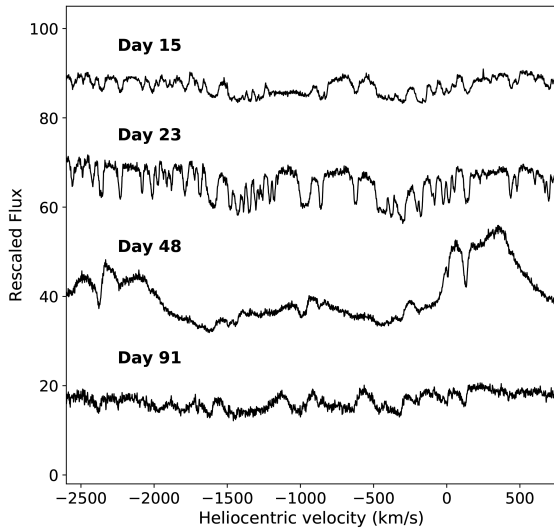


**Figure 2.** Evolution of ASASSN-17hx in the region of  ${}^7\text{Be}$ . Spectra are in heliocentric velocities with the zero of the scale set at  ${}^7\text{Be II } \lambda 313.0583 \text{ nm}$ .

Monai & Beers (2000). Our spectra provide an independent estimate of the reddening from the diffuse interstellar band (DIB) at 578.0 nm using the relation of Friedman et al. (2011). We measure an EW of the DIB of 0.05797 nm that implies  $E(B - V) = 1.139 \text{ mag}$ . Adopting this value and  $E(G_{\text{BP}} - G_{\text{RP}}) = 0.41595A_V$ ,<sup>1</sup> we derive a colour for the likely nova progenitor ( $G_{\text{BP}} - G_{\text{RP}} = -0.202 \text{ mag}$ , which corresponds to a black-body with a temperature of about 17 000 K.

The UVES spectra of ASASSN-17hx have been taken at four epochs starting from day 15 after the maximum at JD 245 7964.4886 until day 91. The region around  ${}^7\text{Be}$  at these epochs is shown in Fig. 2. The spectra of day 15 and day 23 are very similar but quite different from the other epochs. In the early spectra, common features are strong absorptions with relatively low velocity at  $\approx -300$  and  $\approx -450 \text{ km s}^{-1}$  and a broad high-velocity component spanning  $200 \text{ km s}^{-1}$  with a mean velocity at  $\approx -1000 \text{ km s}^{-1}$ .

The spectrum of day 23 is shown in the left panel of Fig. 3 where the  ${}^7\text{Be II}$ , Ca II K, Fe II  $\lambda 516.90 \text{ nm}$  and H $\gamma$  regions are plotted on to a common velocity space. A close correspondence could be found only for the  $-450 \text{ km s}^{-1}$  component, as marked in the figure. However, the correspondence is lost for the other absorptions and we conclude that  ${}^7\text{Be II}$  is probably not present in the spectrum of the nova outburst. The spectra of later epochs look quite different, showing a marked evolution of the outburst. The spectrum at day 48 is shown in the right panel of Fig. 3. In addition to the  $-460 \text{ km s}^{-1}$  component, it shows the presence of a new and very strong component at  $-700 \text{ km s}^{-1}$ , while the very-high-velocity component has vanished. In the last epoch, the new component has decreased considerably, although remaining quite strong, and has moved slightly to  $\approx -800 \text{ km s}^{-1}$ . In both these epochs, no correspondence is found between Ca II and a possible presence of  ${}^7\text{Be}$  and we conclude that there is no evidence for the presence of  ${}^7\text{Be II}$  in the spectrum. Because of the general weakening of the absorption, there are several absorption features that can be identified in the  ${}^7\text{Be}$  regions as Cr II lines of 313.668, 313.206 and 312.870 nm. This supports the conclusion that  ${}^7\text{Be II}$  is either weak

or totally absent. Of the few novae investigated so far, this is the first nova for which it is possible to rule out, with some confidence, the presence of  ${}^7\text{Be II}$  in the outburst spectra. The failure to detect  ${}^7\text{Be}$  should have an important bearing on the thermonuclear mechanisms leading to the  ${}^7\text{Be}$  synthesis and ejection.

## 2.2 Nova Mus 2018

Nova Mus 2018, also PNV J11261220–6531086, was discovered on 2018 January 14 by Rob Kaufman (2018, AAVSO Alert Notice 609) in the Musca constellation with a visual magnitude of  $\approx 7.0 \text{ mag}$ , and then confirmed as a Fe II nova. Archival data of ASASSN Sky Patrol observations show that the nova eruption began approximately two weeks earlier (P. Schmeer, AAVSO Alert Notice 609). The light curve of Nova Mus 2018 is shown in Fig. 1.

Nova Mus 2018 faded quite rapidly and we are able to take four epochs, which include one epoch on the maximum brightness and the other three covering up to 45 d after maximum when the nova was already of 14 mag, just before the beginning of the observed dust formation dip. The nova became a very difficult target for observations at  ${}^7\text{Be II } \lambda 313.1 \text{ nm}$  and the spectra at days 40 and 45 are severely underexposed in the region. The early spectra are shown in Fig. 4. The spectrum at day 35 in the  ${}^7\text{Be II}$  region is compared with the Ca II K, Fe II  $\lambda 516.903 \text{ nm}$  and H $\gamma$  lines in Fig. 5. The spectrum shows a relatively simple structure with three main absorption components at  $-820$ ,  $-920$  and  $-1150 \text{ km s}^{-1}$  and a number of smaller ones. All these components have a clear correspondence with the stronger of the  ${}^7\text{Be II } 313.1$  doublet and often show evidence for the fainter one as well. A zoom of the spectrum of Nova Mus 2018 at day 35 is shown in Fig. 6. Thus, there are no doubts about the identification and we consider it to be a robust detection of  ${}^7\text{Be II}$ .

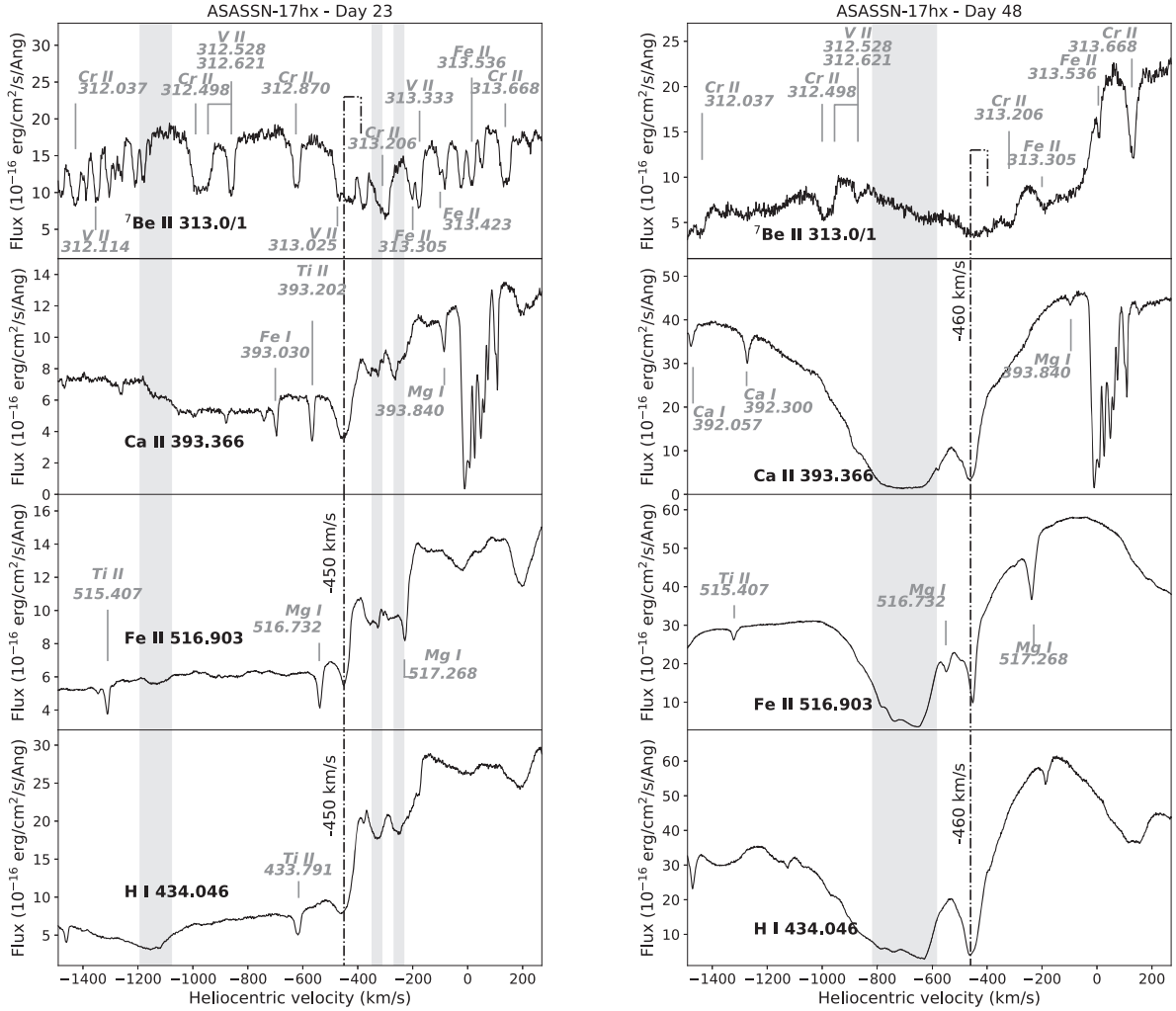
## 2.3 Nova Cir 2018

Nova Cir 2018, also PNV J13532700–6725110, was discovered by John Seach on 2018 January 19, in the constellation of Circinus. The nova brightened slowly from magnitude  $V \approx 8.5$  to 6.3 mag by January 27. Then it fluctuated between magnitudes  $V \approx 6.5$  and 8.5 mag for about three months, before fading to below magnitude  $V \approx 9 \text{ mag}$  on June 25, as can be seen from its light curve shown in Fig. 1. Spectroscopic observations obtained on January 30 show a number of Fe II lines with absorption troughs at about  $-1300 \text{ km s}^{-1}$  (Strader et al. 2018a). SALT optical spectroscopy also reported a component at  $-500 \text{ km s}^{-1}$  (Aydi et al. 2018).

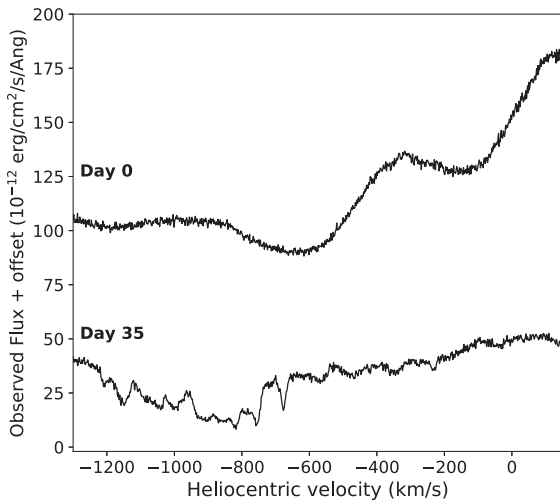
The evolution of the spectral features around the  ${}^7\text{Be II } \lambda 313.1 \text{ nm}$  region is shown in Fig. 7. At day  $-15$  from the maximum taken at JD 245 8157.0024, there is a huge absorption spanning more than  $1000 \text{ km s}^{-1}$ , which in the observation at day 12 breaks down into two main absorption features centred at  $-400$  and  $-1500 \text{ km s}^{-1}$ , respectively. Later observations show relatively little change in the profile, with the main absorption feature shifting to higher expansion velocities. It is only in the relatively late spectra, because of the weakening of the absorption, that some fine structure becomes visible.

Fig. 8 shows the  ${}^7\text{Be II}$  region compared, in velocity space, with other lines for days 66 and 75. At first glance, there is some possible  ${}^7\text{Be}$  absorption corresponding in velocity to the Ca II K features. However, the peak intensity does not correspond precisely and most of the absorption could be ascribed to Cr II. In particular, there are narrow features, which become visible only at this stage, without corresponding features of the weaker of the  ${}^7\text{Be II}$  doublet. Thus,

<sup>1</sup>See <http://stev.oapd.inaf.it/cgi-bin/cmd>; this value is derived using the O'Donnell (1994) extinction curve.



**Figure 3.** Left: spectrum of ASASSN-17hx at day 23 in the region of  $^7\text{Be}$  II, compared with the Ca II K, Fe II  $\lambda$ 516.903 nm and H $\gamma$  lines. All identifications shown in the panels refer to the  $-450 \text{ km s}^{-1}$  component. At zero and slightly positive velocities, there are multiple components as a result of the interstellar Ca II K line. Right: the spectrum of the nova at day 48. Note that at this epoch the main absorption component is found at  $-460 \text{ km s}^{-1}$ . The x-axis is the same as in Fig. 2.



**Figure 4.** Evolution of Nova Mus 2018 in the region of  $^7\text{Be}$ . The x-axis is the same as in Fig. 2.

we conclude that  $^7\text{Be}$  is possibly absent or very weak in the outburst spectra of this nova.

#### 2.4 Nova ASASSN-18fv

ASASSN-18fv is an exceptionally bright nova discovered in the Carina constellation on 2018 March 20 (Stanek et al. 2018), by the ongoing ASASSN. It reached  $V \approx 6$  mag on March 22. The light curve is characterized by substantial jittering above the base level on a time-scale of days. According to the classification by Strope, Schaefer & Henden (2010), it was classified as a J-class nova. ASASSN-18fv was clearly detected by NuSTAR in both the FPMA and FPMB instruments but not in the *Swift* XRT observation (Nelson et al., 2018). The progenitor of ASASSN-18fv was identified by Strader et al. (2018b) in the *Gaia* Data Release 1 (DR1; Prusti et al. 2016) and in the VST Photometric H $\alpha$  Survey (VPHAS) DR2 (Drew et al. 2014). The object in *Gaia* DR1 is at an angular distance of less than  $0'.1$  from the nova, with no other objects in the catalogue within a radius of 5 arcsec. The object is also present in *Gaia* DR2 (Arenou et al. 2018; Brown et al. 2018) that provides a parallax of 0.151 mas with an error of 0.488 mas. It also provides

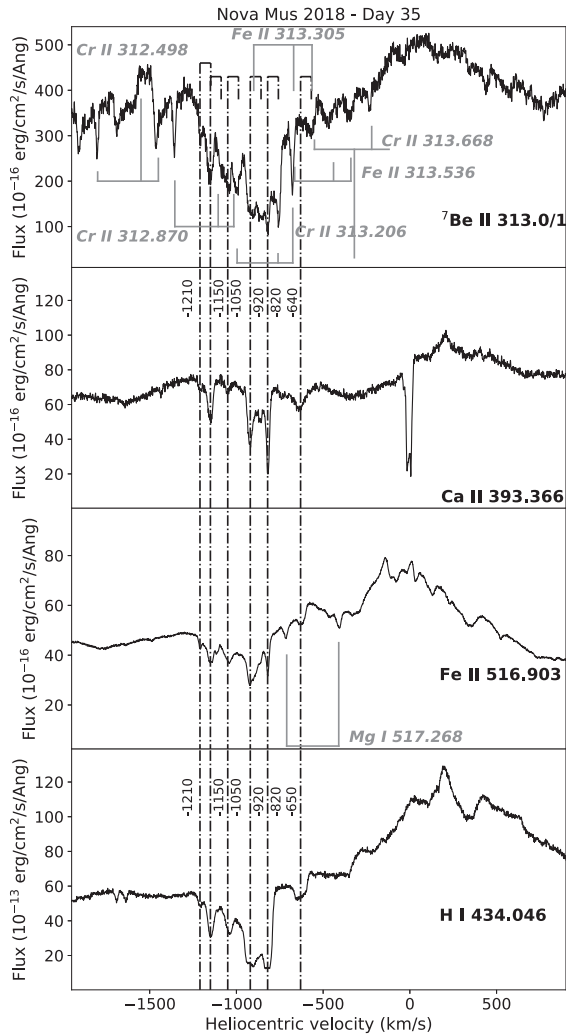


**Figure 5.** Spectrum of Nova Mus 2018 at day 35. The blends identified in the  ${}^7\text{Be II}$  panel refer to the three main components with velocities of  $-820$ ,  $-920$  and  $-1150$   $\text{km s}^{-1}$ , respectively. The x-axis is the same as in Fig. 2.

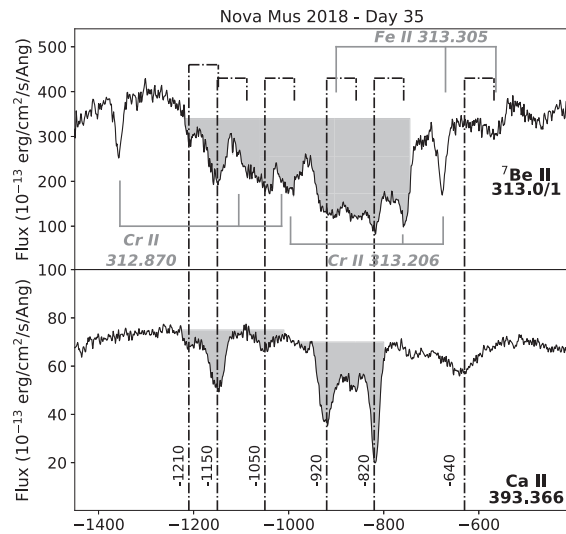


**Figure 6.** Magnification of the spectrum of Nova Mus 2018 at day 35 to show the  ${}^7\text{Be II}$  identifications.

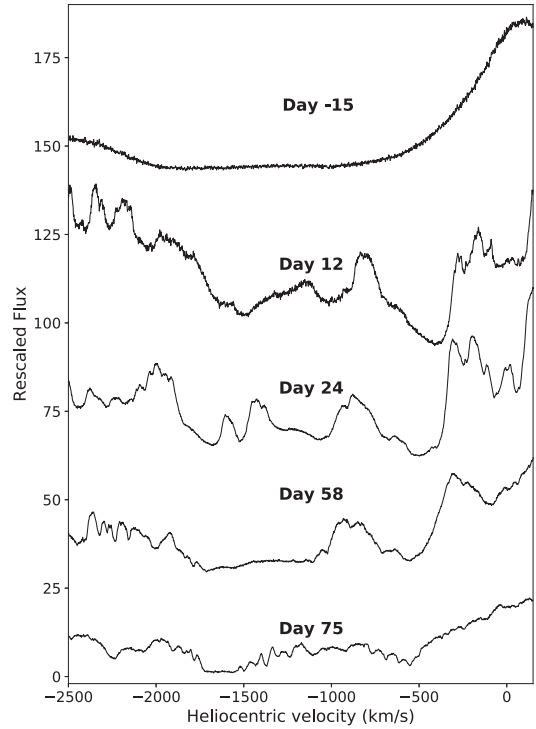


**Figure 7.** Evolution of Nova Cir 2018 in the region of  ${}^7\text{Be}$ . The x-axis is the same as in Fig. 2.

a  $G$  magnitude of 19.688 mag and a colour  $G_{\text{BP}} - G_{\text{RP}} = 0.869$  mag.

We succeeded in triggering the ToO programme on 2018 March 22, achieving one of the few spectra of a nova during its maximum ever taken. A first report of the spectroscopic observations close to the maximum was given in Izzo et al. (2018b). The optical spectrum shows a bright continuum and is characterized by several narrow absorption features and significant Balmer and Paschen jumps. The hydrogen lines, O I 777.3 nm and several multiplets of Fe II are in emission with a P Cygni profile. The main component in absorption is centred at  $v \sim -250$   $\text{km s}^{-1}$ , which is a relatively modest velocity for a nova and suggests a possible peculiar nature.

Our spectra allow us to obtain an independent estimate of the reddening in the direction of the nova. The reddening maps of Schlafly & Finkbeiner (2011) provide  $E(B - V) = 1.1046$  mag for the position of the nova. In our spectra, we were able to detect several interstellar features. The velocity span by the Na I D lines and the Ca II H&K lines was much smaller than the span by the H I 21-cm emission. This strongly suggests that the light from the nova goes through only a part of the Galactic interstellar medium along that line of sight. The Na I D lines are saturated and not well suited to estimating the reddening, so we used the DIB at 578.0 nm instead. We measure an EW of 0.01917 nm that, using the relations of Friedman et al. (2011), implies  $E(B - V) = 0.37$  mag (i.e.  $A_V = 1.15$  mag), in good agreement with the value from the maps of Schlafly & Finkbeiner (2011). Adopting this value and  $E(G_{\text{BP}} - G_{\text{RP}}) = 0.41595A_V^2$  we thus derive a colour for the nova progenitor ( $G_{\text{BP}} - G_{\text{RP}}) = 0.39066$  mag that corresponds to a black-body of about 8200 K.

<sup>2</sup>See <http://stev.oapd.inaf.it/cgi-bin/cmd>; this value is derived using the O'Donnell (1994) extinction curve.

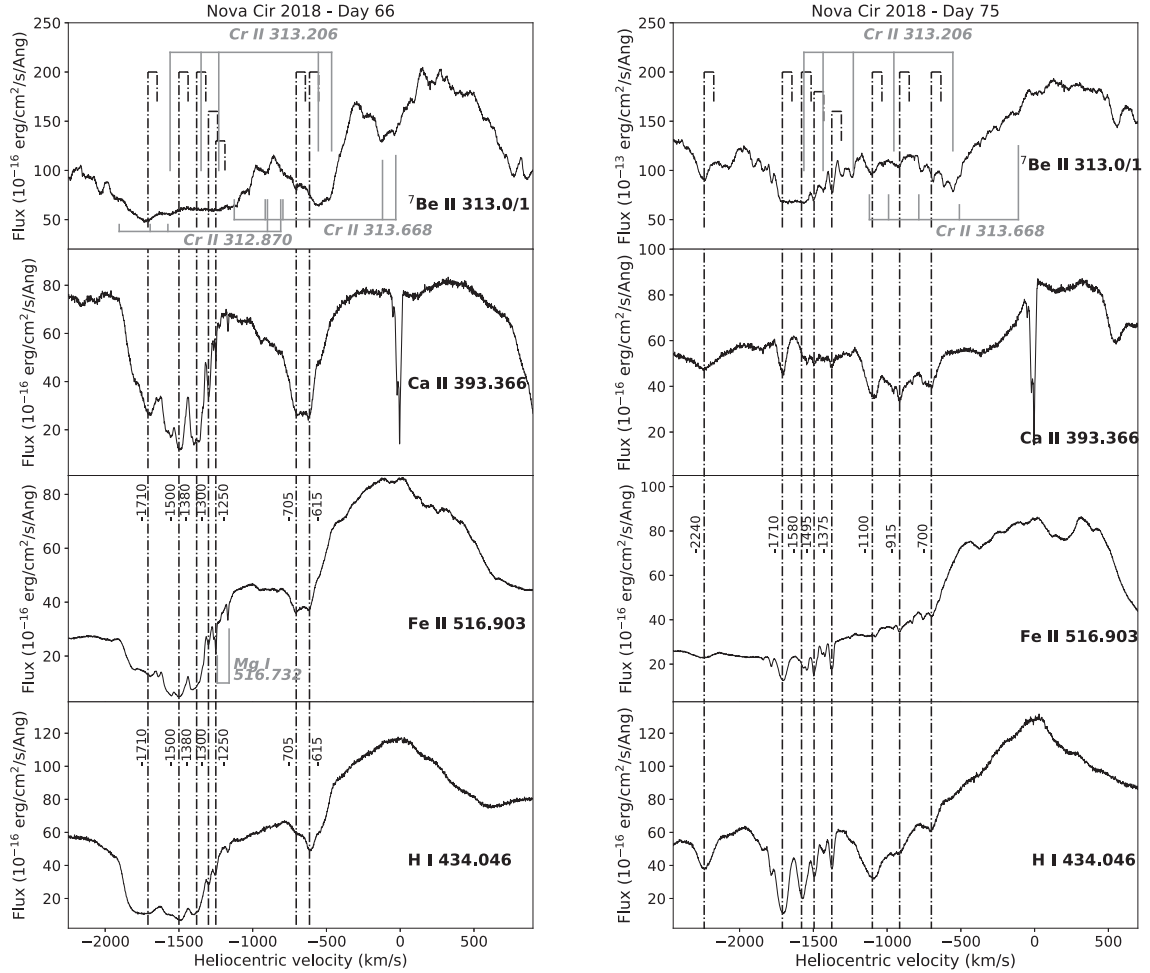


**Figure 8.** Spectra of Nova Cir 2018 at day 66 in the left panel and at day 75 in the right panel. The Cr II blends identified in the  ${}^7\text{Be}$  II panel refer to the five main components with velocities of  $-615$ ,  $-705$ ,  $-1380$ ,  $1500$  and  $-1710$   $\text{km s}^{-1}$ , respectively.

In early epochs, the UVES spectral region around  ${}^7\text{Be}$  shows a broad unresolved absorption. The main contribution is possibly  ${}^7\text{Be}$  II but it cannot be proved. It is only for epochs later than day 63 that the weakening of general absorption reveals structure and the  ${}^7\text{Be}$  doublet can be recognized in several discrete components, as can be seen in Fig. 9. The day 98 spectrum is plotted in Fig. 10 and shows five discrete components at  $-395$ ,  $-490$ ,  $-780$ ,  $-805$  and  $-880$   $\text{km s}^{-1}$ , respectively. Corresponding to these components, there is a feature at the position of the  ${}^7\text{Be}$  II  $\lambda 313.0583$  nm line and also in several components of the  ${}^7\text{Be}$  II  $\lambda 313.1228$  nm line. A magnification of the spectrum of this epoch is shown in Fig. 11. At this epoch, the  ${}^7\text{Be}$  decay has reduced by a factor of 2–3 the original abundance contributing to the blanketing reduction in the region. The components of the other lines present in the region as the Cr II 312.870, 313.206 and 313.668 nm lines also become visible.

### 3 ${}^7\text{BE}$ ABUNDANCE ESTIMATE

The  ${}^7\text{Be}$  abundance in the nova ejecta can be estimated relatively to Ca, which is not a nova product. Single ionization is the main stage for both species in the expanding shell with no evidence of neutral or double ionized stages. However, column densities can be derived with confidence only when discrete and unsaturated components are seen. These are not always present in the outburst

spectra and sometimes a sequence of observations lasting about 100 d from maximum are required for their detection (Molaro et al. 2016). Moreover, the presence of several blends and the possibility of emissions make the placement of the continuum in the  ${}^7\text{Be}$  II region quite problematic. To reduce the effects of possible contaminants, it is convenient to measure the sum of the  ${}^7\text{Be}$  II  $\lambda 313.0583 + \lambda 313.1228$  doublet and to compare it with the Ca II K line at 393.366 nm, which is relatively free from blends. The  $\log(gf)$  of the  ${}^7\text{Be}$  II doublet are  $-0.178$  and  $-0.479$ , and that of Ca II K is  $+0.135$ . Following Spitzer (1998), we can write

$$\frac{N({}^7\text{Be II})}{N(\text{Ca II})} = 2.164 \times \frac{W({}^7\text{Be II, doublet})}{W(\text{Ca II, K})}. \quad (1)$$

The Nova Mus 2018 spectrum in the regions of  ${}^7\text{Be}$  II and Ca II K line at day 45 is shown in Fig. 6. A major contaminant is Cr II, and the expected positions of the strongest lines of Table 3 are marked in the figure. The component at  $-820$   $\text{km s}^{-1}$  of Cr II 313.668 nm is identified. The same component of Cr II 313.206 is strong and has an EW of 96 mÅ. The components at  $-920$  and  $-1150$   $\text{km s}^{-1}$  should be present but blended with the  ${}^7\text{Be}$  II absorption. Also marked in the figure are the components of the Cr II 312.870 nm line. However, the  $-1150$   $\text{km s}^{-1}$  component should be visible if present and, therefore, this line is very weak. The Cr II 312.498 nm and the Cr II 312.036 lines are seen in all the main velocity components.

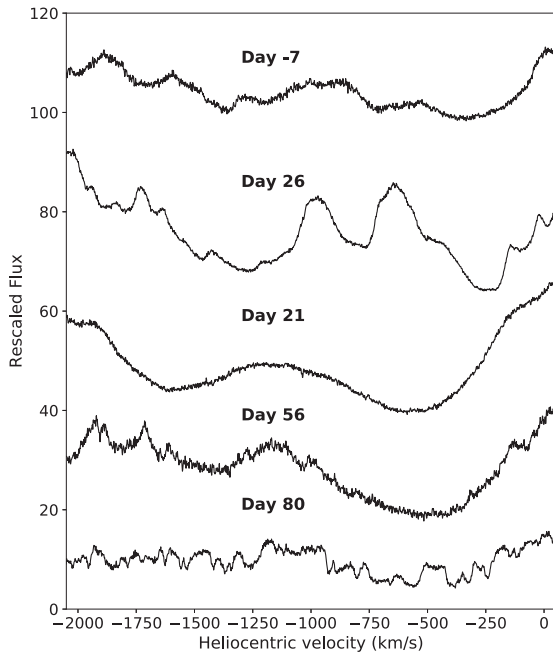


**Figure 9.** Spectral evolution of ASASSN-18fv in the region of  ${}^7\text{Be}$ . Only a selection of spectra corresponding to the major spectral changes are shown for sake of clarity. The x-axis is the same as in Fig. 2.

By scaling with the relative strength, we estimate that the EWs of the Cr II components blended within the  ${}^7\text{Be}$  II absorption are of 160 mÅ from Cr II 313.206 and of  $\approx 40$  mÅ from Cr II 312.870 nm. The EW of the whole region spanned by the  ${}^7\text{Be}$  II components is of  $1.8 \pm 0.150$  Å with blends taken into account. The main uncertainty comes from the continuum placement with a possible error of about 10 per cent. However, the Ca II 393.3 nm line is free of blends and the local continuum can be also determined with confidence. The EW of the Ca II 393.3 nm line is of  $0.910 \pm 0.030$  Å providing a ratio of  $\text{EW}({}^7\text{Be II})/\text{EW}(\text{Ca II}) = 1.98$ . Note that by using the component at velocity  $-1150$  km s $^{-1}$  alone and the stronger of the  ${}^7\text{Be}$  III doublet, we would obtain a ratio of  $\text{EW}({}^7\text{Be II}_{313.0583})/\text{EW}(\text{Ca II}) = 1.22$ . This is equivalent to a ratio of 1.83 for the whole  ${}^7\text{Be}$  absorption and consistent with the ratio derived by using the integral of the whole absorption including all components. With equation (1), we obtain  $N({}^7\text{Be II})/N(\text{Ca II}) = 4.28 (\pm 0.4)$ .  ${}^7\text{Be}$  is unstable with a half life of 53.2 d. Thus, the abundance at explosion has been reduced by a factor of 1.6 after 35 d. Assuming a solar abundance of  $\text{Ca II}/\text{H} = 2.18 \times 10^{-6}$  (Lodders et al. 2009), we obtain in Nova Mus 2018 an abundance of  ${}^7\text{Be}/\text{H} = 1.5 \times 10^{-5}$ . The calcium abundance is assumed to be solar in all cases considered here. Should Ca be higher than solar, the final  ${}^7\text{Be}/\text{H}$  would decrease accordingly.

The ASASSN-18fv UVES spectrum at day 98 is shown in Fig. 10. There are five discrete and narrow Ca II K components and all have the corresponding  ${}^7\text{Be}$  II 313.0583 nm and 313.1228 nm lines. At this epoch, the contaminants can also be seen and Cr II 312.8700 nm, Cr II 313.2053 nm and Cr II 313.6681 nm are identified in the figure. The ratio between the shadowed area of Be II and Ca II in Fig. 11 is  $\text{EW}({}^7\text{Be})/\text{EW}(\text{Ca II}) = 1.52$ . Similar ratios are measured also at day 63, 81 and 86. Thus,  $N({}^7\text{Be II})/N(\text{Ca II}) = 3.29$ , by number. Considering the  ${}^7\text{Be}$  decay, the original abundance becomes a factor of 3.0 larger, i.e.  $N({}^7\text{Be II})/N(\text{Ca II}) = 9.9$ . Assuming also here that all of Ca and  ${}^7\text{Be}$  are singly ionized and solar abundances for

calcium, we obtain in ASASSN-18fv an abundance of  ${}^7\text{Be}/\text{H} = 2.15 \times 10^{-5}$ .

#### 4 DISCUSSION

The present detection of  ${}^7\text{Be}$  in the outburst spectra of ASASSN-18fv and Nova Mus 2018 provides additional evidence that  ${}^7\text{Be}$  is freshly created in the thermonuclear runaway via the reaction  ${}^3\text{He}(\alpha, \gamma){}^7\text{Be}$  and ejected during nova explosion. Nova Mus 2018 is a fast nova while ASASSN-18fv is moderately fast, according to the Gaposchkin (1957) classification, showing that the  ${}^7\text{Be}$  production is not related to the kind of nova. This is consistent with what is observed in the sample of novae studied so far with a mixture of different nova types and uncorrelated  ${}^7\text{Be}$  abundances.

In ASASSN-17hx and possibly also in Nova Cir 2018, there is no clear evidence for the presence of  ${}^7\text{Be}$  in the outburst spectrum. These are the first novae where the  ${}^7\text{Be}$  isotope has not been detected since it has been searched for. This shows that the thermonuclear reaction chain taking place on the WD and the ejection phase could be quite complex. The  ${}^7\text{Be}$  produced in the thermonuclear runaway chain needs to be transported relatively quickly to the surface by convection. This is a sort of Cameron–Fowler mechanism invoked for Li-rich red giants (Cameron & Fowler 1971) and it may not always operate effectively. The turbulent turnover time-scales are of the order of 100 s throughout the initial deflagration stage. Therefore, at the same time as the temperature is driving the convection, the mixing may be incomplete within the shell (Shore 2019). We note also that in the latest numerical simulations of Starrfield et al. (2019) the  ${}^7\text{Be}$  yields are very sensitive to the WD mass, decreasing by a factor of 30 from the most massive WD to the lighter WDs.

The extant  ${}^7\text{Be}/\text{H}$  measurements are summarized in Table 3. The abundances derived in Nova Mus 2018 and ADSASSN18xv are comparable with those derived in V339 Del (Tajitsu et al. 2015), V838 Her (Selvelli et al. 2018) and V2944 Oph (Tajitsu et al. 2016) but a factor of 3 lower than those obtained in V407 Lup (Izzo et al. 2018a) and a factor of 5 lower than in V5668 Sgr (Molaro et al. 2016).

We emphasize that  ${}^7\text{Be}/\text{H}$  remains larger by at least one order of magnitude than predicted by nova models (Starrfield et al. 1978; Hernanz et al. 1996; José & Hernanz 1998). We note, however, that the final amount of  ${}^7\text{Be}$  is sensitive to the amount of  ${}^3\text{He}$  in the donor star as a higher abundance of  ${}^3\text{He}$  is expected to result in a higher  ${}^7\text{Be}$  abundance. Boffin et al. (1993) and Hernanz et al. (1996) found a logarithmic dependence of the  ${}^7\text{Be}$  output to the initial  ${}^3\text{He}$  abundance. The non-linearity of  ${}^7\text{Be}$  yields results from  ${}^3\text{He}({}^3\text{He}, 2p){}^4\text{He}$  and its importance increases as the square of the initial  ${}^3\text{He}$  abundance. Therefore, it produces a leaking of the available  ${}^3\text{He}$  for the  ${}^3\text{He}(\alpha, \gamma){}^7\text{Be}$ , whose rate increases only linearly for the initial  ${}^3\text{He}$  abundance. For  ${}^3\text{He}$  enhancements up to 100 solar, Boffin et al. (1993) derive  $X({}^7\text{Be})/X({}^7\text{Be}_0) = 1 + 1.5 \log X({}^3\text{He})/X({}^3\text{He}_0)$ , where  ${}^7\text{Be}_0$  is the  ${}^7\text{Be}$  final mass fraction obtained with a solar initial  ${}^3\text{He}$  mass fraction. From the theoretical point of view, it is believed that low-mass main-sequence stars synthesize  ${}^3\text{He}$  through the p–p chains with peak abundances of few  $10^{-3}$  by number (Iben 1967). As the star ascends, the red giant branch convection dredges up  ${}^3\text{He}$ -enriched material to the surface, which is later expelled into the interstellar medium by wind or during the planetary phase.  ${}^3\text{He}$  is a particularly difficult element to measure. It can be measured in H II regions by using

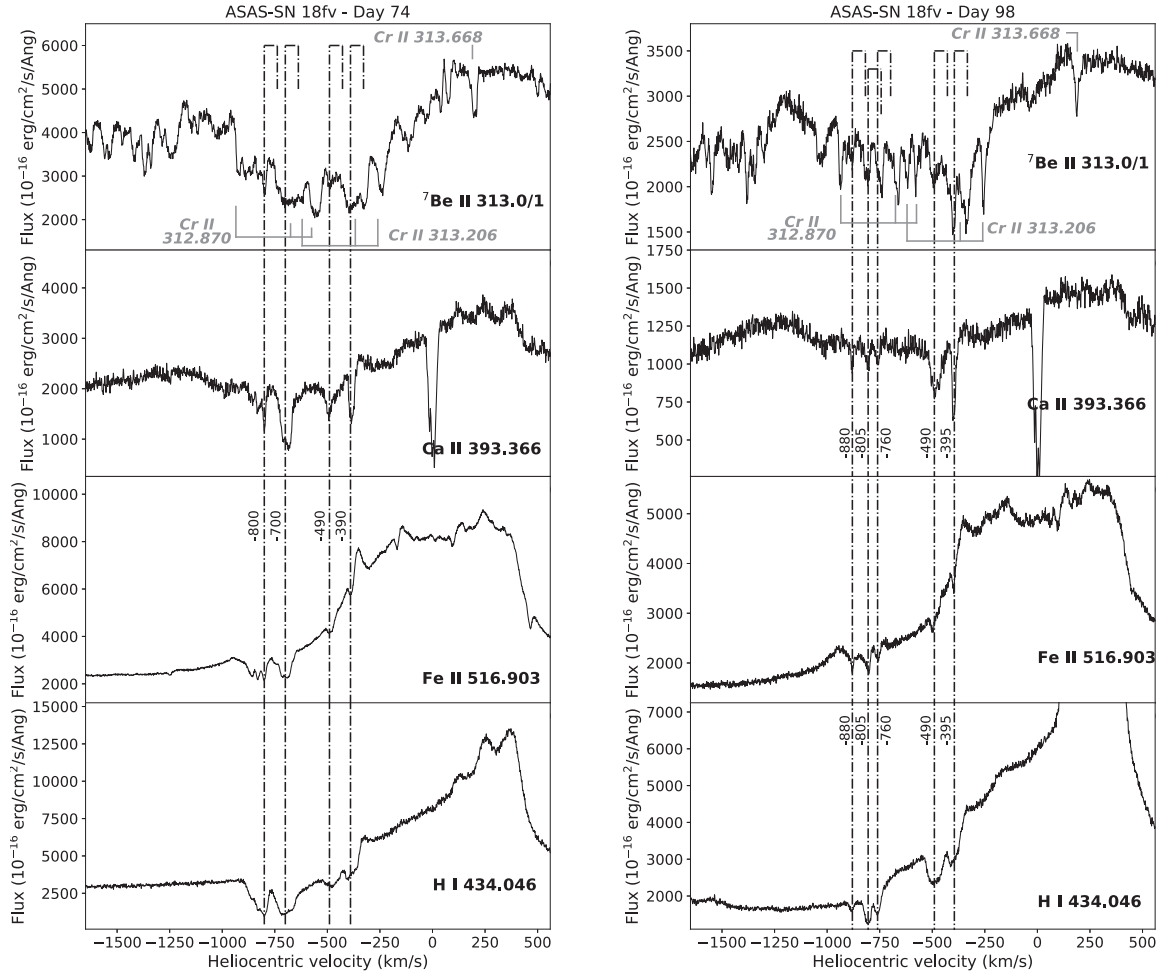


**Figure 10.** Spectra of ASASSN-18fv at day 98. The blends identified in the  $^7\text{Be}$  II panel refer to the three main components with velocities of  $-390$ ,  $-490$  and  $-700$   $\text{km s}^{-1}$ , respectively.

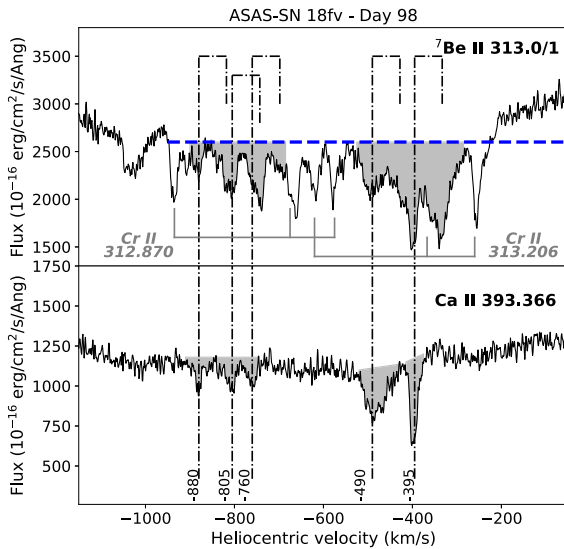


**Figure 11.** Magnification of the spectrum of day 98 of ASASSN-18fv. The shadowed regions show the area used for the equivalent widths.

**Table 3.** The  $^7\text{Be}/\text{H}$  (number) for the novae with narrow absorption components. The original values from Tajitsu et al. (2015, 2016) are corrected here for the decay of  $^7\text{Be}$ . References are: (1) Tajitsu et al. (2015); (2) Molaro et al. (2016); (3) Izzo et al. (2018a); (4) Tajitsu et al. (2016); (5) Selvelli et al. (2018); (6) this paper.

Nova	Type	Day	Comp	$^7\text{Be}/\text{H}$	Ref.
V339 Del	CO	47	$-1103$	$1.9 \times 10^{-5}$	1
		47	$-1268$	$3.2 \times 10^{-5}$	1
V5668 Sgr	CO	58	$-1175$	$1.7 \times 10^{-4}$	2
		82	$-1500$	$1.3 \times 10^{-4}$	2
V2944 Oph	CO	80	$-645$	$1.6 \times 10^{-5}$	4
V407 Lup	ONe	8	$-2030$	$6.2 \times 10^{-5}$	3
V838 Her				$2 \times 10^{-5}$	5
ASASSN-17hx				None	6
Nova Mus		35	All	$1.5 \times 10^{-5}$	6
Nova Cir				Uncertain	6
ASASSN-18fv		80	All	$2.2 \times 10^{-5}$	6

measurements at a frequency of 8.665 GHz (i.e. 3.46 cm), which is emitted naturally by ionized  $^3\text{He}$  (Bania, Rood & Balser 2010; Balser & Bania 2018) or in the stellar atmospheres of hot stars (Geier et al. 2012). Surprisingly, interstellar medium observations indicate that there is far less of this element in the Galaxy than the current

models predict. In order not to overproduce  ${}^3\text{He}$  in the course of chemical evolution, it has become customary to assume that some unknown  ${}^3\text{He}$ -destruction mechanism is at work in low-mass giants (Dearborn, Steigman & Tosi 1996; Galli et al. 1997; Chiappini, Renda & Matteucci 2002; Romano & Matteucci 2003). For instance, Charbonnel & Zahn (2007) suggested a thermohaline mixing during the red giant branch phase of low-mass stars. However, in a few planetary nebulae,  ${}^3\text{He}/\text{H}$  is found to be high at the level of  $10^{-3}$ , consistent with predictions from standard stellar models (Rood, Bania & Wilson 1992; Balser & Bania 2018).

Novae are semi-detached binary systems in which a Roche lobe filling secondary star transfers material to the WD primary. In the Roche geometry, there is a direct relation between the orbital period and the mass of the secondary star (Warner 1976; Knigge 2006), that, in the case of novae, gives M2 values close to  $0.3 M_{\odot}$ . Because stars with mass lower than  $0.3 M_{\odot}$  are fully convective, the  ${}^3\text{He}$  produced in the core by the incomplete pp1 chain is transported outward and transferred to the WD surface. If the donor star has  ${}^3\text{He}$  much greater than the solar value, this would almost reconcile the observations with the model predictions.

${}^7\text{Be}$  decays via electron capture into  ${}^7\text{Li}$  with a half-life of 53.22 d. However, despite the temporal span of our observations, which in some cases extend up to more than 100 d, we do not detect the  ${}^7\text{Li}$  I  $\lambda\lambda 670.8$  nm absorption line at the corresponding positions of other neutral lines, such as Na I D doublet and Ca I  $\lambda 422.7$  nm, which are observed. We do not detect any  ${}^7\text{Li}$  I  $\lambda\lambda 670.8$  nm absorption corresponding to the main components of Nova Mus 2018. A possible weak feature is detected in the very early spectrum of Nova ASASSN-18fv, as shown in Fig. 12. So far, the  ${}^7\text{Li}$  I  $\lambda 670.8$  nm line has been detected only in the early spectra of Nova Cen 2013 (Izzo et al. 2015). This shows that the physical conditions in the ejecta sometimes permit the survival of neutral  ${}^7\text{Li}$  I at least in the very early stages. However, this cannot be the result of  ${}^7\text{Be}$  decay as it is close to the nova outburst. As argued by Molaro et al. (2016), the  ${}^7\text{Be}$  decays via capture of an internal K electron resulting in  ${}^7\text{Li}$  II, which has no lines in the optical spectral range and therefore is not observable. The non-detection of  ${}^7\text{Li}$  in the later outburst spectra implies that the ejected gas had been heated and that almost all Li remains ionized.

The typical atomic fraction  ${}^7\text{Be}/\text{H}$  of  $\approx 2 \times 10^{-5}$  corresponds to a  ${}^7\text{Li}$  overabundance of four orders of magnitude with respect to the meteoritic value of  ${}^7\text{Li}/\text{H} \approx 2 \times 10^{-9}$  (Lodders et al. 2009). With an ejecta of  $\approx 10^{-5} M_{\odot}$ , a nova event is producing a  ${}^7\text{Li}$  mass of  $1.4 \times 10^{-9} M_{\odot}^{\text{Li}}$  and, with a nova rate of 50 novae  $\text{yr}^{-1}$  over  $10^{10}$  yr, a total  ${}^7\text{Li}$  mass of  $700 M_{\odot}^{\text{Li}}$ , which is a considerable fraction of the estimate of about  $1000 M_{\odot}^{\text{Li}}$  for the Galaxy (Cescutti & Molaro 2019). The precise fraction contributed by novae is related to uncertainties in the nova rate and to the behaviour of the rate in the course of Galactic life. However, the primordial  ${}^7\text{Li}$  production is between  $\approx 80 M_{\odot}^{\text{Li}}$ , when taking the halo star abundance, and  $250 M_{\odot}^{\text{Li}}$ , when taking the predicted value of primordial nucleosynthesis with the baryon density of the deuterium abundance or cosmic microwave background. The contribution by galactic cosmic rays is about  $8 M_{\odot}^{\text{Li}}$  as estimated indirectly by  ${}^9\text{Be}$ , which is produced by the same processes (Molaro et al. 1997). The contribution of the AGB stars is about  $1 M_{\odot}^{\text{Li}}$ , which is negligible (Rukeya et al. 2017). The nova  ${}^7\text{Li}$  production has been considered by means of a detailed model of the chemical evolution of the Milky Way by Cescutti & Molaro (2019). They showed that novae could account for the observed increase of  ${}^7\text{Li}$  abundances with increasing of metallicity in the thin disc. The agreement of the model with the Li abundances is obtained for a delay time for the nova production of  $\approx 1$  Gyr and

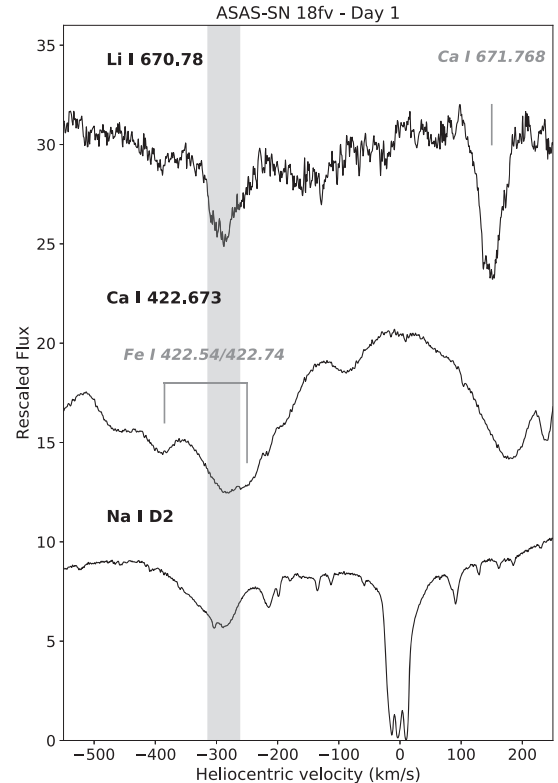


**Figure 12.** Spectrum of ASASSN-18fv at day 1 showing the presence of the absorption feature of  ${}^7\text{Li}$  I  $\lambda 670.8$  nm, observed at the same expanding velocity of  $v = -290 \text{ km s}^{-1}$  as the resonance line of Ca I  $\lambda 422.673$  nm, though blended with Fe I  $\lambda 422.74$  nm, and the Na I D2 absorption. On the top spectrum, the component at  $-290 \text{ km s}^{-1}$  of Ca I  $\lambda 671.768$  nm is also marked. This further supports the presence of the neutral species in this component.

of  $1.8(\pm 0.6) \times 10^{-5} M_{\odot}^{\text{Li}}$  of  ${}^7\text{Li}$  as effective yields for a whole nova life, which is consistent with the mean  ${}^7\text{Be}$  observed. With  $\approx 10^4$  nova events during a lifetime, this corresponds to  $1.8 \times 10^{-9} M_{\odot}^{\text{Li}}$  per event, which is consistent with what is obtained here. Despite all the uncertainties, novae appear as the dominant source and the only one able to account for the bulk of Galactic  ${}^7\text{Li}$ .

## 5 CONCLUSIONS

Following the recent detection of  ${}^7\text{Be}$  II in the outburst spectra of classical novae, we started a ToO project at the ESO with the high-resolution spectrograph UVES to search for the  ${}^7\text{Be}$  isotope in all bright novae. The nova brightness is required to study the resonance doublet lines  ${}^7\text{Be}$  II at  $\lambda\lambda 313.0583, 313.1228$  nm where the atmospheric absorption is strong and optical elements of the spectrograph have low efficiency. We observed all four bright novae of the last two years. We summarize the main results here.

(i) The  ${}^7\text{Be}$  II doublet absorption lines are detected in two novae, Nova Mus 2018 and ASASSN-18fv, confirming the synthesis of  ${}^7\text{Be}$  in the nova thermonuclear runaway. The atomic fractions by number are estimated to be  $X({}^7\text{Be})/X(\text{H}) \approx 1.5 \times 10^{-5}$  and  $2.2 \times 10^{-5}$  in Nova Mus 2018 and ASASSN-18fv, respectively, when the  ${}^7\text{Be}$  decay is taken into account. There are seven novae where the  ${}^7\text{Be}$  abundance has been measured. Five of them have a  ${}^7\text{Be}/\text{H}$  abundance close to  $\approx 2 \times 10^{-5}$  while two show higher values. The value of  $\approx 2 \times 10^{-5}$  looks like a typical abundance, though the sample remains rather small.

(ii) We do not detect  ${}^7\text{Be}$  II lines in the spectra of ASASSN-17hx and possibly not in Nova Cir 2018 either. This shows that not all novae eject  ${}^7\text{Be}$ . Theoretically, it is expected that the  ${}^7\text{Be}$  yields decrease with the decrease of the WD mass. The yields decrease by a factor of 45 passing from 1.35 to 0.6  $M_{\odot}$  for the WD (Starrfield et al. 2019). Moreover, very little  ${}^7\text{Be}$  is produced in the case of reduced mixing between the WD core products with the material of the donor star, and the absence of  ${}^7\text{Be}$  could reveal such an occurrence. The present fraction of novae showing no evidence of  ${}^7\text{Be}$  is of 22 per cent. Note that Mason et al. (2020) recently suggested that ASASSN-17hx could not be a classical nova or at least a very peculiar one. If this is the case, the absence of  ${}^7\text{Be}$  would have a very specific meaning.

(iii) The  ${}^7\text{Be}/\text{H}$  abundance of  $\approx 2 \times 10^{-5}$  is higher by about one order of magnitude than the predictions of nova models. We argue that a higher than solar abundance of  ${}^3\text{He}$  in the donor star would result in higher  ${}^7\text{Be}$  yields. In fact,  ${}^3\text{He}/\text{H} \approx 10^{-3}$ , one hundred times the solar abundance as observed in few planetary nebulae by Balsa & Bania (2018), could be common in the small mass donor stars, thus producing a factor of 4 increase in the  ${}^7\text{Be}$  yields. This would reduce significantly the disagreement between the observations and the nova models.

(iv) A  ${}^7\text{Be}/\text{H}$  abundance of  $\approx 2 \times 10^{-5}$  implies a  ${}^7\text{Li}/\text{H}$  overproduction of  $\approx 4$  dex above the meteoritic value. A simple estimation based on the mass ejecta and nova rate shows that they are likely the missing  ${}^7\text{Li}$  source required to account for 75–90 per cent of  ${}^7\text{Li}$  in the Milky Way.

## ACKNOWLEDGEMENTS

We gratefully acknowledge Elena Mason and Gabriele Cescutti for helpful discussions on the interpretation of the data. We thank an anonymous referee for many useful comments. We also thank Gabriella Schiulaz for checking the English language. LI was supported by grants from VILLUM FONDEN (project numbers 16599 and 25501). Based on observations collected at the European Southern Observatory under ESO programmes 299.D-5043, 0100.D0621, 0102.D-0284.

## REFERENCES

Arenou F. et al., 2018, *A&A*, 616, A17  
 Arnould M., Norgaard H., 1975, *A&A*, 42, 55  
 Aydi E., Buckley D. A. H., Mohamed S., Whitelock P. A., 2018, *The Astronomer's Telegram*, 11287  
 Balsa D. S., Bania T. M., 2018, *AJ*, 156, 280  
 Bania T. M., Rood R. T., Balsa D. S., 2010, in Charbonnel C., Tosi M., Primas F., Chiappini C., eds, *Proc. IAU Symp. Vol. 268, Light Elements in the Universe*. Kluwer, Dordrecht, p. 81  
 Boffin H. M. J., Paulus G., Arnould M., Mowlavi N., 1993, *A&A*, 279, 173  
 Bonifacio P., Monai S., Beers T. C., 2000, *AJ*, 120, 2065  
 Brown A. G. A. et al., 2018, *A&A*, 616, A1  
 Cameron A. G. W., Fowler W. A., 1971, *ApJ*, 164, 111  
 Cescutti G., Molaro P., 2019, *MNRAS*, 482, 4372  
 Charbonnel C., Zahn J.-P., 2007, *A&A*, 467, L15  
 Chiappini C., Renda A., Matteucci F., 2002, *A&A*, 395, 789  
 Dearborn D. S. P., Steigman G., Tosi M., 1996, *ApJ*, 465, 887  
 Drew J. E. et al., 2014, *MNRAS*, 440, 2036  
 Friedjung M., 1979, *A&A*, 77, 357  
 Friedman S. D. et al., 2011, *ApJ*, 727, 33  
 Galli D., Stanghellini L., Tosi M., Palla F., 1997, *ApJ*, 477, 218  
 Gaposchkin C. H. P., 1957, *The Galactic Novae*. North-Holland, Amsterdam  
 Geier S., Heber U., Edelman H., Morales-Rueda L., Kilkenny D., O'Donoghue D., Marsh T. R., Copperwheat C., 2012, in Kilkenny D., Jeffery C. S., Koen C., eds, *ASP Conf. Ser. Vol. 452, Fifth Meeting*

on Hot Subdwarf Stars and Related Objects. *Astron. Soc. Pac.*, San Francisco, CA, p. 57  
 Gomez-Gomar J., Hernanz M., Jose J., Isern J., 1998, *MNRAS*, 296, 913  
 Guarro J. et al., 2017, *The Astronomer's Telegram*, 10737  
 Harris M. J., Teegarden B. J., Weidenspointner G., Palmer D. M., Cline T. L., Gehrels N., Ramaty R., 2001, *ApJ*, 563, 950  
 Hernanz M., Jose J., Coc A., Isern J., 1996, *ApJ*, 465, L27  
 Iben I. J., 1967, *ARA&A*, 5, 571  
 Izzo L. et al., 2015, *ApJ*, 808, L14  
 Izzo L. et al., 2018a, *MNRAS*, 478, 1601  
 Izzo L. et al., 2018b, *The Astronomer's Telegram*, 11468  
 José J., Hernanz M., 1998, *ApJ*, 494, 680  
 Knigge C., 2006, *MNRAS*, 373, 484  
 Lawler J. E., Sneden C., Nave G., Den Hartog E. A., Emrahoğlu N., Cowan J. J., 2017, *ApJ*, 228, 10  
 Lodders K., Palme H., Gail H.-P., 2009, *Landolt–Börnstein, New Series, Astronomy and Astrophysics*. Springer, Berlin  
 Mason E., Shore S. N., Kuin P., Bohlens T., 2020, *A&A*, preprint ([arXiv:2001.11747](https://arxiv.org/abs/2001.11747))  
 Molaro P., Bonifacio P., Castelli F., Pasquini L., 1997, *A&A*, 319, 593  
 Molaro P., Izzo L., Mason E., Bonifacio P., Della Valle M., 2016, *MNRAS*, 463, L117  
 Munari U., Ochner P., Hamsch F.-J., Frigo A., Castellani F., Milani A., Valisa P., Vagnozzi A., 2017, *The Astronomer's Telegram*, 10736  
 Nelson T., Mukai K., Sokoloski J. L., Metzger B., Chomiuk L., Linford J., Vurm I., 2018, *The Astronomer's Telegram*, 11608  
 O'Donnell J. E., 1994, *ApJ*, 422, 158  
 Pavana M., Anupama G. C., Selvakumar G., Kiran B. S., 2017, *The Astronomer's Telegram*, 10613  
 Poggiani R., 2018, *The Golden Age of Cataclysmic Variables and Related Objects IV (GOLDEN 2017)*, preprint ([arXiv:1807.07947](https://arxiv.org/abs/1807.07947))  
 Prusti T. et al., 2016, *A&A*, 595, A1  
 Romano D., Matteucci F., 2003, *MNRAS*, 342, 185  
 Rood R. T., Bania T. M., Wilson T. L., 1992, *Nature*, 355, 618  
 Rukeya R., Lü G., Wang Z., Zhu C., 2017, *PASP*, 129, 074201  
 Schlafly E. F., Finkbeiner D. P., 2011, *ApJ*, 737, 103  
 Schlegel D. J., Finkbeiner D. P., Davis M., 1998, *ApJ*, 500, 525  
 Selvelli P., Molaro P., Izzo L., 2018, *MNRAS*, 481, 2261  
 Shappee B. J. et al., 2014, *ApJ*, 788, 48  
 Shore S. N., 2019, in Werner K., Stehle C., Rauch T., Lanz T., eds, *ASP Conf. Ser. Vol. 519, Radiative Signatures from the Cosmos*. *Astron. Soc. Pac.*, San Francisco, CA, p. 161  
 Siebert T. et al., 2018, *A&A*, 615, A107  
 Spitzer L., 1998, *Physical Processes in the Interstellar Medium*. Wiley, New York  
 Stanek K. Z. et al., 2017a, *The Astronomer's Telegram*, 10387  
 Stanek K. Z. et al., 2017b, *The Astronomer's Telegram*, 10436  
 Stanek K. Z. et al., 2017c, *The Astronomer's Telegram*, 10523  
 Stanek K. Z. et al., 2018, *The Astronomer's Telegram*, 11454  
 Starrfield S., Bose M., Iliadis C., Hix W. R., Woodward C. E., Wagner R. M., 2019, *ApJ*, submitted, preprint ([arXiv:1910.00575](https://arxiv.org/abs/1910.00575))  
 Starrfield S., Iliadis C., Hix W. R., 2016, *PASP*, 128, 051001  
 Starrfield S., Truran J. W., Sparks W. M., Arnould M., 1978, *ApJ*, 222, 600  
 Strader J., Chomiuk L., Holoien T. W. S., Prieto J. L., Stanek K. Z., Shappee B. J., Dong S., 2018b, *The Astronomer's Telegram*, 11456  
 Strader J., Chomiuk L., Swihart S., Shishkovsky L., 2018a, *The Astronomer's Telegram*, 11209  
 Strope R. J., Schaefer B. E., Henden A. A., 2010, *AJ*, 140, 34  
 Tajitsu A., Sadakane K., Naito H., Arai A., Aoki W., 2015, *Nature*, 518, 381  
 Tajitsu A., Sadakane K., Naito H., Arai A., Kawakita H., Aoki W., 2016, *ApJ*, 818, 191  
 Warner B., 1976, in Eggleton P., Mitton S., Whelan J., eds, *Proc. IAU Symp. Vol. 73, Structure and Evolution of Close Binary Systems*. Kluwer, Dordrecht, p. 85  
 Williams S. C., Darnley M. J., 2017, *The Astronomer's Telegram*, 10542

This paper has been typeset from a  $\text{\TeX}/\text{\LaTeX}$  file prepared by the author.